Orientation in molecule - surface interactions

1996 J. Phys.: Condens. Matter 8 3245

(http://iopscience.iop.org/0953-8984/8/19/002)

J. Phys.: Condens. Matter **8** (1996) 3245–3269. Printed in the UK

REVIEW ARTICLE

Orientation in molecule–surface interactions

U Heinzmann†, S Holloway‡, A W Kleyn§, R E Palmer‖ and K J Snowdon¶

† Universität Bielefeld, Fakultät für Physik, Universitätsstrasse 25, 33501 Bielefeld, Germany
‡ Surface Science Research Centre, University of Liverpool, Liverpool L69 3BX, UK
§ FOM Institute for Atomic and Molecular Physics, Kruislaan 407, 1098 SJ Amsterdam, The Netherlands
‖ Nanoscale Physics Research Laboratory, School of Physics and Space Research, University of Birmingham, Edgbaston, Birmingham B15 2TT, UK
¶ Department of Physics, University of Newcastle, Newcastle upon Tyne NE1 7RU, UK

Received 9 February 1996

Abstract. The role of the orientation of a molecule in its interaction with a surface is examined for a number of cases. At first the determination of the static orientation of a molecule at the surface is discussed. A dependence of the orientation on state and coverage is found for O_2 molecules adsorbed on Ag(110). The orientation dependence of NO in chemisorption, displacement reactions, and chemical reactions is discussed. Rotational excitation of NO in collisions with surfaces is shown to exhibit a strong orientation dependence. Dissociative chemisorption of hydrogen molecules is found to depend on the initial orientation of the molecule. Finally, in dissociative collisions of fast molecules with surfaces the role of the initial orientation is examined and the final orientation of the molecular axis is determined. Several mechanisms for molecular dissociation are discussed.

1. Introduction

The macroscopic rates and outcome of many important processes in present day technology such as those occurring during the manufacturing of semiconductor devices, the modification of materials and in heterogeneous catalysis depend ultimately on the interactions between individual atoms and molecules and specific sites on solid surfaces. Detailed studies of the kinematics and dynamics of the interactions on the atomic scale are therefore of considerable practical relevance. The macroscopic rates and outcome of such processes depend critically on the microscopic kinematics and dynamics of the interactions on the atomic scale. Studies of the kinematics have been carried out for several decades already. The study of the dynamics of such interactions is a new rapidly growing field of pure research. The interaction of molecules with surfaces is dependent on:

—the molecule–surface separation;
—the lateral position of the molecule within the surface unit cell;
—the molecular orientation;
—the velocity of the molecule;
—the angular momentum of the molecule;
—the vibrational state of the molecule; and
—the electronic state of the molecule.

0953-8984/96/193245+25$19.50

To this list we must add the substrate degrees of freedom such as phonons, plasmons and electron–hole pairs and recognize the possible influence of steps and defects. It is clear that obtaining a full theoretical description which includes all degrees of freedom is a formidable task. One approach may be to choose model systems for which the influence of certain degrees of freedom is minimized (e.g., the lateral position of the molecule on close-packed crystal surfaces). Alternatively, the influence of those degrees of freedom over which we can exert considerable control could be systematically investigated. However, since the positions and velocities of the nuclei and the electronic state of the system change throughout the interaction of a molecule with a surface, and it is not possible to follow this development continuously, we can at best hope to infer the detailed dynamics of the interaction from a series of 'snapshots' of the system, before, during and after the interaction.

Recently, experimental methods have become available to study the molecular orientational degree of freedom of the molecule. We are now able to prepare molecules in a preferred orientation before the collision and to analyse the molecular orientation after a collision event. This paper describes recent progress in understanding the influence of the molecular orientation on the equilibrium configuration of molecules adsorbed on surfaces, on intramolecular and molecule–surface energy transfer, and on molecule reactivity at and dissociative and non-dissociative scattering behaviour from surfaces.

It is well known that molecules are adsorbed on surfaces with preferential orientations [1–3]. Such preferred orientations ultimately reflect the response of the molecule to the orientation dependence of the potential energy surface describing the interaction. The fact that molecules eventually adsorbed are oriented with respect to the surface cannot, however, be taken as evidence that the dynamics of gas–surface interactions is governed by the initial molecular orientation in the gas phase. For example, at very low energies the molecule might be expected to achieve its optimum orientation adiabatically during its approach to the surface, independent of its initial orientation. Alternatively, the oriented chemisorption state on the surface may be reached by first trapping into a precursor state, a process which itself might not show a significant orientational preference. Such preferences, if they exist at all, may in fact have more to do with the influence of the initial orientation on the dissipation of the translational energy of the incident molecule, a necessary prerequisite for adsorption.

Several experimental studies have given indirect evidence for the possible importance of steric effects in adsorption [4–8]. It has also been suggested that an analysis of the orientation and possibly also the rotational distribution of scattered (initially randomly oriented) molecules may reveal the influence of orientation on adsorption [8–11]. For example, an orientation dependence of dissociative adsorption, caused by an orientation-dependent activation barrier, should deplete the scattered beam of those orientations most energetically favoured for dissociative chemisorption. However, as for adsorption, orientational anisotropies in the scattered beam may be a simple consequence of an orientation dependence of energy and momentum transfer between the translational and internal degrees of freedom of the molecule.

Recently, the importance of the orientation coordinate in gas–surface interactions has been demonstrated directly, both in scattering experiments with initially oriented molecules and in dissociative and non-dissociative scattering experiments in which the orientation distributions of correlated fragments and scattered molecules were measured. In this report we present the results of a coordinated investigation of such phenomena for the interaction of diatomic molecules with crystal surfaces. In the first section of the paper we discuss the determination of the molecular orientation of an adsorbed molecule. Having learned about the equilibrium adsorbate orientation we will focus our attention on the

orientation dependence of the adsorption step itself and on the dependence on the initial orientation of the reactivity of molecules incident on surfaces. For a better understanding of such adsorption studies we follow with a theoretical investigation of the dynamics of the interaction of an initially oriented molecule with a surface. Finally, measurements of the fragment orientation distributions of dissociatively scattered energetic molecules are presented. Our discussion spans the incident molecule energy range from 0.1 eV to several keV. Due to the different properties of the various experimental techniques used, the research described in this report is not limited to a single molecule, but studies on several simple diatomic molecules such as H_2, D_2, O_2, N_2 and NO will be presented.

2. Orientation of adsorbed molecules

One of the principal questions which we need to ask in seeking to understand the role of molecular orientation in the molecule–surface interaction is 'what is the connection between the orientation of the molecule as it approaches (or leaves) the surface and the orientation of the molecule in the adsorbed state?' Experimental studies of the orientation of adsorbed molecules are now well established [3], although it turns out that the systems which have been extensively addressed in surface crystallographic studies are not necessarily the same systems whose dynamical behaviour has been of most interest. Here we will consider the recent application of surface structural techniques to determine the molecular orientation in a system of particular interest to the dynamics community, O_2/Ag(110). Very recently a number of molecular beam scattering and adsorption studies have been carried out for the O_2/Ag system; see, e.g., [12–22]. This system is important because it manifests three distinct adsorption states: physisorbed O_2 ($T < 40$ K), molecularly chemisorbed O_2 (40 K $< T <$ 180 K) and atomically chemisorbed O ($T > 180$ K) [23, 24]. The molecularly chemisorbed state is regarded as a precursor to dissociative adsorption, and, similarly, the physisorbed state is regarded as a precursor to intact molecular chemisorption. One of the most striking features of the dynamical behaviour of this system is the very low sticking coefficient for O_2 on Ag(110) at liquid nitrogen temperatures (i.e. into the molecularly chemisorbed state, possibly via the physisorbed precursor), $<10^{-3}$ [12–14, 22]. By contrast, the sticking coefficient into the physisorbed state at $T \sim 30$ K appears to approach unity [23]. Even more significantly, when the physisorbed layer is warmed up, the efficiency of conversion into the molecularly chemisorbed state is high, perhaps 50%. These results present a paradox—two different experiments which seem to measure the probability of sticking into the molecularly chemisorbed state give two quite different results.

A possible (and intriguing) resolution of this paradox is suggested by recent structural studies of O_2/Ag(110) and associated molecular dynamics simulations. The orientation of the chemisorbed O_2 molecule is generally held to be parallel to the surface with the axis along the [1 −1 0] direction (i.e. parallel to the troughs on the Ag(110) surface) [25]. However, recent near-edge x-ray absorption fine-structure (NEXAFS) measurements [23] indicate that the orientation of the physisorbed molecule at monolayer coverage is different, with the axis approximately parallel to the surface but pointing along the [001] direction—figure 1—perpendicular to the chemisorbed molecule and to the troughs on the surface. This orientation is reproduced by molecular dynamics simulations [26]. Significantly, these simulations indicate that the molecule–molecule interaction stabilizes the orientation of physisorbed O_2 along [001] at monolayer coverage; the ground state of the isolated, physisorbed O_2 molecule is, in fact, along the troughs, just like that of the chemisorbed molecule.

One appealing interpretation of these results is as follows. The probability that a

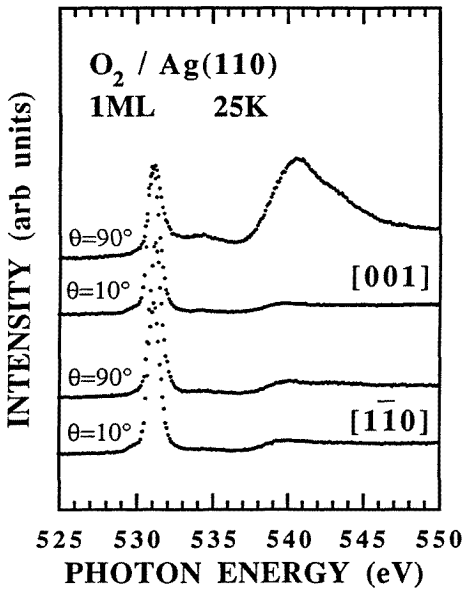

Figure 1. High-resolution NEXAFS spectra of one monolayer of physisorbed O_2/Ag(110) taken at near grazing and normal incidence along the high-symmetry azimuths. These results show that the molecular axis is oriented parallel to the surface in the [001] direction, perpendicular to the established orientation of the chemisorbed molecule [23].

physisorbed O_2 molecule perpendicular to the rows converts into a chemisorbed O_2 species along the rows is high, whereas the probability that a physisorbed O_2 molecule oriented along the rows converts is low. In other words, the topology of the molecular potential energy surface is such that conversion of the physisorbed to the chemisorbed state is favoured if the physisorbed molecule is oriented perpendicular to the chemisorbed species. This optimum orientation of the physisorbed precursor is stabilized by the O_2–O_2 interaction in the physisorbed layer, whereas the sticking experiments at 80 K correspond to the limit of zero coverage as far as the physisorbed state is concerned, and here the orientation discriminates against conversion into the chemisorbed state. If this interpretation is correct, it represents striking evidence of the key role played by the molecular orientation in molecule–surface dynamics, a role which is likely to extend well beyond the model system of O_2/Ag(110).

A second example of an experiment which probes the interplay between the orientation of an adsorbed molecule and the 'orientational dynamics' of the molecule–surface interaction is provided by recent studies [27] of electron-stimulated desorption (ESD) of negative ions [28] from physisorbed O_2/graphite. This adsorption system has been intensively studied, and a rich variety of surface structural phases have been identified. In particular, at $T \sim 25$ K, it is possible to prepare two monolayer phases: the δ-phase, in which the molecular axes are approximately parallel to the surface, and the $\zeta 2$-phase, in which the molecules stand up [29]. However, the angular distributions of ions desorbed from these two phases as a result of electron beam impact are almost identical—each shows a peak normal to the surface; see figure 2. This behaviour contrasts with what is observed in many chemisorbed systems, where the angular distribution seems to manifest the orientation of the molecule on the surface—the basis of the 'ESDIAD' technique [30]. In short, the reason for this correlation breaking down in a physisorbed system is that the energy difference ($\sim$10 meV) between the two different orientations on the surface (and, indeed, the binding energy of the molecule to the surface, $\sim$100 meV) is minimal when compared with the energy pumped into the system by the impinging particle (the electron energy is $\sim$10 eV). Molecular dynamics simulations [27] indicate that the process of ion desorption

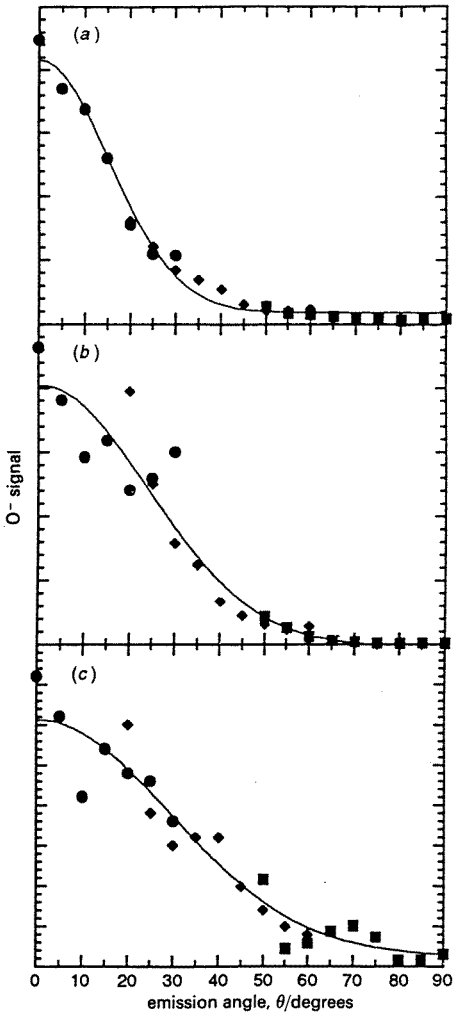

Figure 2. Angular distributions of O^- ions produced by electron-impact-physisorbed O_2/graphite. (a) The ζ2-phase, electron energy 8 eV; (b) the ζ2-phase, electron energy 20 eV; (c) the δ-phase, electron energy again 20 eV. Note that the angular distributions show a peak normal to the surface irrespective of the initial orientation of the molecule on the surface [27].

is accompanied by significant rotational excitation, so the initial orientational order on the surface is lost; the overall shape of the angular distributions is then governed by the electrostatic image potential experienced by the charged ion as it leaves the surface. On the other hand, the yield of desorbed ions does depend very significantly on the initial orientation of the molecule on the surface. Once again, these results indicate not only that the molecular orientation is an important factor in the surface dynamics but also that we cannot presume there to be a simple relationship between the orientation of the molecule when adsorbed on the surface and the favoured orientation of the molecule (or, in this case, the favoured trajectories of the molecular fragments) above the surface. Direct measurements of the orientation dependence of surface processes are necessary.

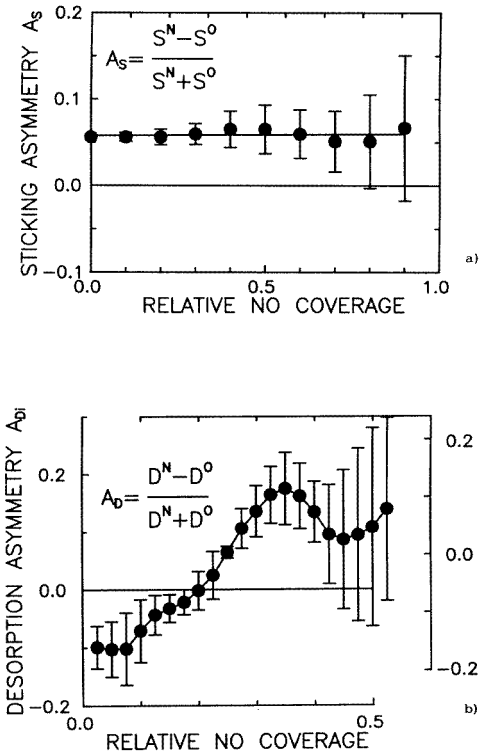

Figure 3. Orientation asymmetry of the (a) NO sticking and (b) CO desorption at CO/Ni(100) as a function of NO coverage. In (b) the left-hand asymmetry scale refers to each incoming NO molecule, the right-hand scale to each sticking NO molecule. In contrast to the cases described in figures 4 and 5 the degree of orientation of the NO molecules was only 12.6% in this experiment [47].

3. Preparation of oriented molecule beams

In oriented-beam experiments, a (pulsed) supersonic molecular beam of NO (seeded in Ne and He) is used to provide beams in which nearly all molecules will be in the lowest rotational level of the $\Pi_{1/2}$ electronic ground state of NO. Due to the linear Stark effect, an electric hexapole focusing technique produces a beam of state-selected NO molecules, which are subsequently oriented in an electric field perpendicular to the surface [31, 32]. The probability distribution of the specific orientation γ_E of the molecular axis, pointing from O to N, with respect to the electric field direction $\boldsymbol{E}$, can be calculated for the molecules in the selected state ($^2\Pi_{1/2}$, $J = 1/2$, $\Omega = 1/2$, $M_J = 1/2$), and is given by the expression $W(\cos\gamma_E) = 0.5 + 0.5\cos\gamma_E$. This corresponds to a degree of orientation of 33%, given by quantum mechanics as an upper limit. This limit has practically been obtained and used for experiments on the steric effects [33, 34]; the calibration takes place via measurements of the steric effect of sticking, scattering or chemical reaction as a function of the field strength in front of the crystal surface. The field strengths used are high on a laboratory scale (>10 kV cm^{-1}), but very small on an atomic scale. Thus the interaction dynamics at the surface is not affected by the presence of the field.

The translational energy of the NO molecules is varied by means of the composition

of the seed gas (Ar, H_2 and He) to lie between 100 and 350 meV [35]. The sticking coefficients are experimentally determined by the technique of King and Wells [36] using mass spectrometry where all non-sticking molecules as well as the desorbed and the catalytically produced new molecules are detected by means of different mass analysers or a quantum-state-specific REMPI (resonantly enhanced multi-photon ionization) detector. Experiments have been performed concerning the sticking [31, 37–43] and the direct scattering of NO [9, 33, 34, 37, 41, 44–46]. The displacement of pre-adsorbed CO by NO [47], as well as the NO/CO reaction [48] to CO_2 have been measured as a function of the spatial orientation of NO, the NO velocity, the target temperature and the CO versus NO coverages. Single-crystal surfaces of Ag(111) [9, 34, 38–40, 42, 44–46, 49], Ni(100) [31, 33, 47], Pt(100) [35, 37, 48, 50], Pt(111) [41, 45] and Rh(100) [50] have been used as targets. The measurements of steric effects mentioned have been accompanied by LEED, AES, TDS and work-function studies. Using unoriented NO and CO molecules the reaction dynamics has been studied additionally by means of a multi-mass thermal desorption technique [51], where the reaction mechanism, which is explosive in the case of Pt(100) [52], was studied in a time-resolved manner by sweeping through the whole mass spectrum very quickly and thus gaining complete information on the course of the reaction, and thus recording a whole range of mass concentrations simultaneously. In addition to the experiments with oriented beams, several complementary studies using unoriented O_2 beams have been carried out as well.

4. Orientation dependence of NO sticking and chemical reaction with CO

The sticking of NO on Ni(100) [31], on Pt(111) [41, 45], and on CO/Ni(100) [33] and the displacement [47] of the oriented pre-adsorbed CO by the gas-phase oriented NO has been measured. Pronounced steric asymmetry effects have been observed and, in particular, sticking takes place preferentially for incident NO with the N atom pointing towards the surface. The dynamical steric effect thus corresponds with what one would intuitively guess from the orientation of the static NO adsorbate. On the other hand its inverse process, the NO scattering, is preferentially observed for O-end collisions. The displacement of CO by NO, both partners being oriented, shows a steric effect with a negative asymmetry (O-end collisions) at high CO and small NO coverages (see the left-hand side of the lower part of figure 5). For these conditions it is dominated by the steric NO-scattering event, where O-end collisions are also preferentially responsible for CO desorption. The CO-desorption asymmetry changes its sign for higher NO coverage ending up with asymmetry values only given by the asymmetry of the primary NO sticking which is shown in the upper part of figure 3.

NO is mobile on Pt(100) and already desorbs at the surface temperatures studied ($-150\ ^\circ\mathrm{C} < T_s < 100\ ^\circ\mathrm{C}$). A substantial asymmetry was found in the initial sticking probabilities corresponding to a steric effect in the combined signal of scattering and desorbing molecules. In addition to the previously discussed temperature and field-strength dependence [37] we have also examined the dependence of the scattering asymmetry on the translational energy of the incident NO molecules in the range from 100 meV to 350 meV. The results [35] are shown in figure 4. The asymmetry determined from the initial sticking coefficient decreases from values of $\simeq 0.25$ to 0.05 with increasing energy. Our results indicate that the NO adsorption proceeds by direct chemisorption as well as by an orientation-dependent trapping into a precursor state for low translational energies.

The catalytic NO–CO reaction was studied for Pt(100) at surface temperatures in the range 100 °C to 140 °C by exposing the crystal initially covered with a saturation layer of

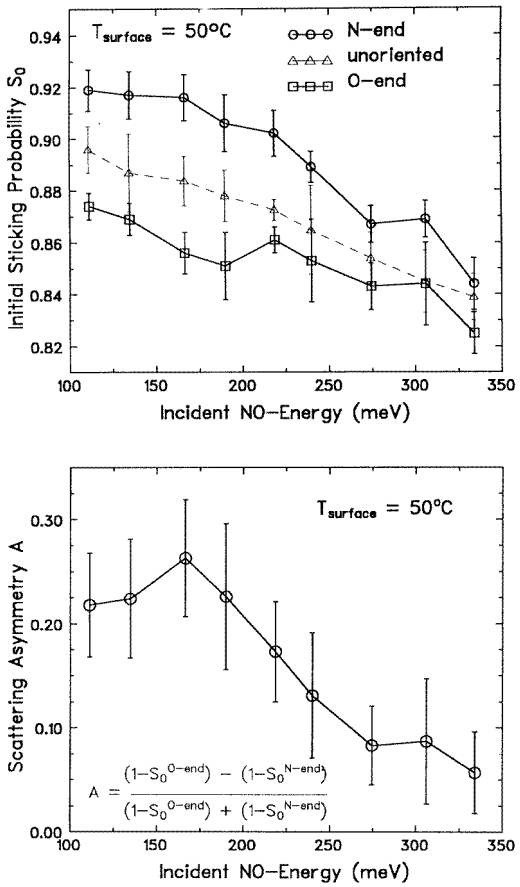

Figure 4. Upper part: the initial sticking probability of NO molecules as a function of the orientation with respect to the Pt(100) surface and of the translational energy; lower part: the corresponding scattering asymmetry defined as given in the inset using the data of the upper part. The NO molecules in the beam had a degree of orientation of 29% in this experiment [35].

CO to the beam of oriented NO molecules and recording simultaneously the CO_2 partial pressure [48, 50]. This signal representing the intensity of the NO–CO reaction shows a maximum as a function of time. Typically, at equal pressures, the reaction proceeds more quickly in the case of preferential N-end collisions, resulting in an initially positive reaction asymmetry which becomes negative at later times (see figure 3). Since CO is not displaced by NO, the NO molecules do not find empty sites at the completely CO-precovered surface directly at the beginning ($t = 0$). The steric effect of the CO_2 reaction, given in figure 5, measured to be positive at high CO and low NO coverages, excludes a description of the catalytic process in terms of a Langmuir–Hinshelwood reaction under these initial conditions. It has to be understood as a direct scattering (Eley–Rideal) effect or as a reaction mechanism via an extrinsic precursor state (Harris–Kasemo) [53]. At lower CO coverages, i.e. later times in figure 5, the chemisorption mechanism starts to dominate the steric effects (Langmuir–Hinshelwood) and the CO_2 reaction asymmetry tends to follow the positive asymmetry values of the sticking process. The details of the reaction asymmetry observed strongly depend on the diffusion of NO on Pt(100) and thus on the crystal temperature. It

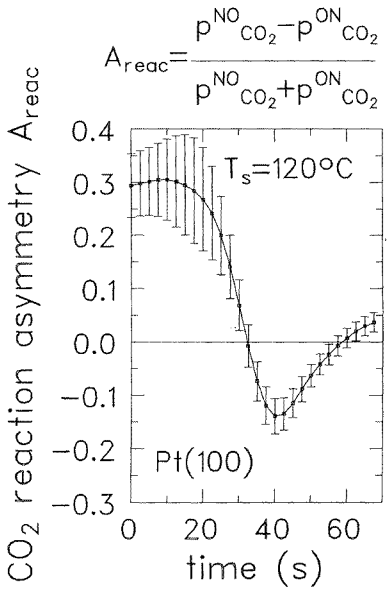

Figure 5. Orientation-dependent CO_2 production asymmetry for the NO–CO reaction on Pt(100) at $T_s = 120$ °C. The NO molecules in the beam had a degree of orientation of 29% in this experiment [48, 50].

is worth noting that similar effects of CO_2 reaction asymmetries have been observed for the NO–CO/Rh(100) complex [50]: high positive reaction asymmetries for zero NO coverage. The interpretation of the time dependencies of the reaction asymmetry for Rh(100) is, however, more complicated than that for Pt(100) because of the CO mobility on the Rh surface and the fact that CO can be partially removed by NO.

5. Scattering of oriented molecules

The scattering experiments making use of oriented beams have been carried out for a number of systems. At first most attention was paid to the interaction of the NO molecule with a fairly inert surface: Ag(111) [9, 34, 38–40, 42, 44–46, 49]. Also the scattering of a variety of polyatomic molecules has been studied; see, e.g., [54–62]. In these experiments the scattered molecules are detected with a quadrupole mass spectrometer or a REMPI detector. For direct scattering of NO from Ag(111) a larger average reflection angle was found for the O-end collision than for the N-end collision [9]. Combining the information from theoretical studies and experiments, it was proposed that the O-end of NO experiences a more anisotropic interaction with the surface [63, 64]. Rotational excitation occurred in a single, impulsive collision at the anisotropic repulsive wall. The rotational excitation spectrum measured for a beam with the O-end oriented towards the surface showed two peaks, the higher one of which is assigned to be a rotational rainbow [34]. When measuring the intensity of the rotational excitation of a molecule resulting from a collision as a function of rotational energy, infinite intensities are found in a classical analysis of the problem. By analogy with atmospheric rainbow scattering, this type of singularity in rotational excitation spectra has been called a rotational rainbow [65–67]. Rotational rainbows were identified first in atom–molecule collisions in the gas phase; see, e.g., [68]. The rainbows are due to

roots of $\partial J/\partial\gamma$ where J denotes the final rotational angular momentum and γ denotes the orientation of the molecular axis with respect to the collision partner.

In the case of a strong attractive well one might expect that a single impulsive collision at the repulsive wall will no longer dominate the interaction. Molecules that get highly rotationally excited will certainly get trapped in the well. For the NO–Pt(111) system the potential well is very deep (1 eV) and sticking is shown to be important up to beam energies of 3 eV and more [69]. The molecule is adsorbed upright in this well with the N end down [70]. Therefore most studies carried out at low beam energies are dominated by trapping/desorption [45, 71]. Experimentally, it is possible to exclude detection of desorbing molecules by time-of-flight techniques or by choosing a low surface temperature T_s [45]. This does not exclude the possibility that the scattered molecules detected for NO–Pt(111) may have moved along very complex trajectories. This has been demonstrated in an extensive experimental and theoretical study on NO scattering from Pt(111) at thermal energies and normal incidence [71, 72]. Rotational rainbows were not observed by Jacobs *et al* when scattering NO from Pt(111) at normal incidence and thermal energies. Haug *et al* have performed quantum mechanical calculations on the NO/Pt(111) system [73]. These authors get good agreement with the experimental data on rotational excitation of Jacobs and Zare using a simple model potential. In addition, the steric effect measured for sticking is also correctly reproduced [38, 41, 45]. The scattering calculations show that rotational rainbows do occur, but are averaged by the surface motion and diluted by trapping in the chemisorption well.

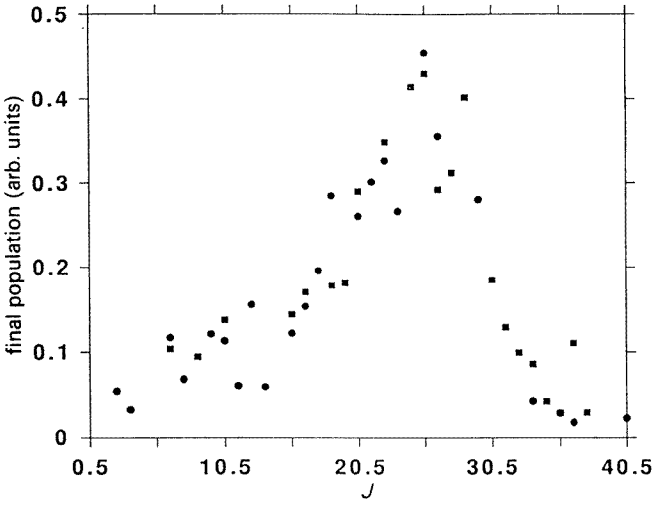

Figure 6. The rotational state distribution for NO scattering from Pt(111) for $E_i = 0.34$ eV, $T_s = 573$ K, $\Theta_i = 45°$, $\Theta_f = 70°$. A maximum at high J (a rotational rainbow) is clearly visible in the spectrum as a peak around $J = 25.5$. From Wiskerke *et al* [75].

Wiskerke *et al* studied rotational excitation in NO scattering from Pt(111) in the energy range from 0.34 eV to 1.6 eV [74–76]. A measured rotational excitation spectrum is shown in figure 6 [75]. The initial energy $E_i = 0.3$ eV, $\Theta_i = 45°$, $\Theta_f = 70°$. Here the incidence angle Θ_i and exit angle Θ_f are measured with respect to the surface normal. The spectrum features a very distinct peak at $J = 25.5$. Both the peak position and the half-height point of the fall-off at high J exhibit a very clear E_i-dependence. Measurements of the

energy transfer carried out using a mass spectrometer show an energy loss of about 50%, a percentage which does not show a strong E_i-dependence [77]. Therefore, we conclude that the peak shown in figure 6 is due to direct inelastic scattering. Comparing this spectrum to the rotational excitation spectrum for NO scattered from Ag(111) with the O end of the NO molecule preferentially oriented towards the surface we find that it shows a striking similarity. Thus it seems very natural to assign the peak observed in figure 6 to a rotational rainbow. Apparently the process that gives rise to the low-J peak for NO/Ag is missing for NO/Pt under otherwise identical conditions. Measurements of the steric effect of direct inelastic scattering of NO from Pt(111) have shown that under the conditions of figure 6 O-end scattering is dominating [41, 45] in contrast to what is observed for NO/Ag(111) [9, 45]. This enhanced scattering for the O end is attributed to enhanced sticking of the molecules with the N end towards the surface. Therefore, the rotational rainbow peak shown in figure 6 will be predominantly due to O-end scattering. The occurrence of a rotational rainbow has also been observed in the CO/Ni(111) system, which also exhibits a deep chemisorption well [8]. In this case the rainbow has been inferred to be due to the O end of the CO molecule. This could not be confirmed by measurements on the steric effects in this system.

At $\Theta_f = 30^\circ$ for low energies and at all Θ_f at the highest energy (1.6 eV) used in the experiment of Wiskerke *et al* the rainbow has disappeared [74, 76]. This can be seen in a Boltzmann plot of some of the data reproduced in figure 7. The rainbow is clearly visible at $\Theta_f = 70^\circ$ for $E_i = 0.34$ eV. At $\Theta_f = 30^\circ$ for the same energy, the high-J peak has disappeared. At higher energies a gradual shift to higher rotational energies and simultaneous disappearance of the peak are observed. At $E_i = 1.6$ eV the rainbow feature has disappeared. Possibly it is overwhelmed at this energy by a broad Boltzmann distribution exhibiting a rotational temperature that clearly exceeds the surface temperature. The Boltzmann distribution might be indicative of a complex interaction in the well as seen in calculations by Jacobs and Zare for NO–Pt(111) and Harris and Luntz for CO–Pt(111) [72, 78].

Very recently, Lahaye *et al* have studied the orientation and energy dependence of the interaction of NO and Pt(111) using classical trajectory calculations [79]. The authors used an interaction potential very similar to that used by Jacobs and Zare [72]. A result of their calculations is also depicted in figure 7. Here it is seen that for exit angles close to the normal, statistical rotational state distributions are found, corresponding to temperatures that are similar to the ones observed experimentally. (Please note that the Θ_f-domain in the calculations is not symmetrical around the experimental Θ_f.) Close to the surface, the rotational state distributions exhibit clearly non-Boltzmann-like rotational excitation, which resembles the experimental results in figure 7.

Lahaye *et al* found that the large rotational excitation is indeed found for O-end scattering. This can be seen in figure 8. Here the rotational excitation is plotted as a function of the initial orientation. The top panel on the left shows rotational excitation for the atop site only. Points are only plotted when sticking does not occur. Around the orientation labelled 1, a cut-off in the rotational excitation is seen. When site and thermal averaging is introduced in the calculation (see the lower panels in figure 8), a maximum in the rotational excitation for O-end orientations is found as well. This is the origin of the rainbow-like peak in simulations and experiment. It is due to scattering with the O end of the molecule, which is purely repulsive. Whether or not this should be strictly referred to rotational rainbow scattering [80] is not addressed by Lahaye *et al*, but the local extremum in the rotational excitation seen is very reminiscent of a rainbow. As the molecule starts rotating after the initial rotational excitation, the N-end approaches the surface and the deep

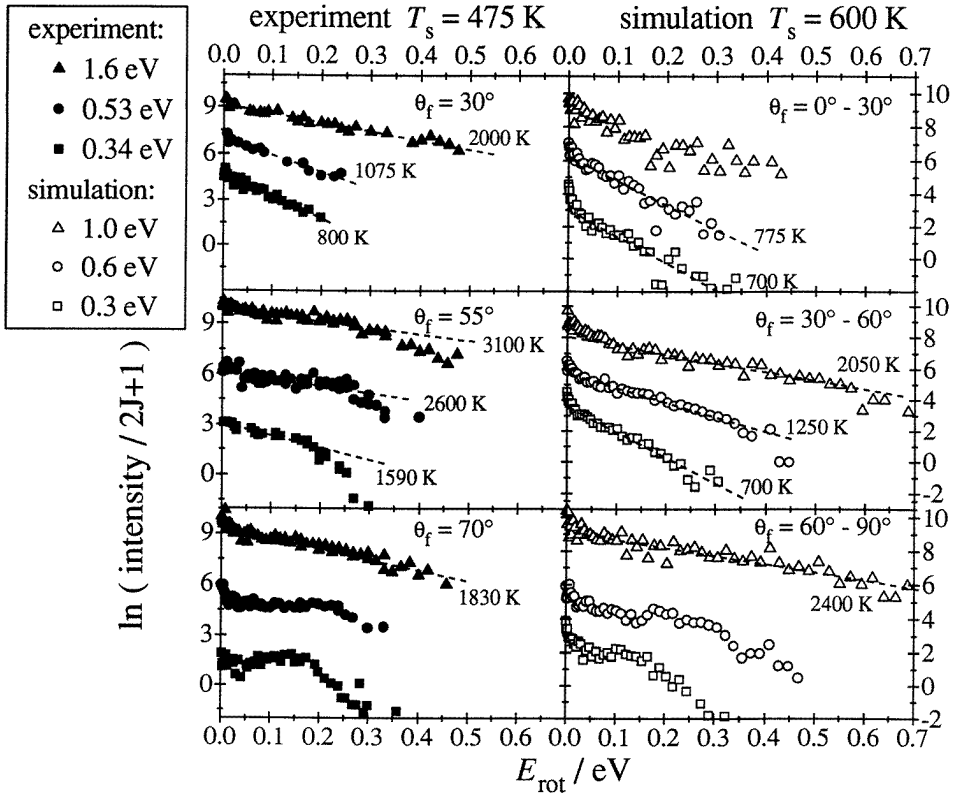

Figure 7. NO scattering from Pt(111) for an incident angle of 45°. The rotational state distribution is plotted as a Boltzmann plot ($\ln(P_f(J)/(2J+1))$ against rotational energy). The left-hand panels contain the experimental data from Wiskerke *et al* [76] and the right-hand panels show the corresponding results of classical trajectory calculations. From top to bottom results for different Θ_f-values (experiment) or different Θ_f-intervals (simulations) are shown. Results for different E_i-values are indicated by different symbols, which are identified in the inset. The temperatures indicated result from the linear least-squares fit though the data points. The scattering of 0.34 eV NO from Pt(111) shows a clear maximum at $\Theta_f = 70°$; the other three distributions appear straight on this Boltzmann plot. From [79].

well is sampled in the trajectory. If a sufficiently deep part of the well is sampled, multiple interactions (chattering) will take place, which often lead to sticking. Thus the molecule is steered away from its originally repulsive orientation into the deep chemisorption well. These multiple interactions are very prominent in this case. Their occurrence has also been studied recently in the Ar–Ag(111) case [81]. It was found that for such a shallow well multiple interactions are not prominent. The maximum of the rotational excitation seen in figure 6 is due to trajectories, where the rotational excitation on the repulsive O-end wall is large, but just not large enough to cause the NO to rapidly reorient and get stuck in the deep N-end potential.

Wiskerke *et al* conjectured that due to reorientation of the molecule when approaching with the O end it would always be captured by the deep N-end well [75]. They proposed a barrier between the two ends of the molecule to prevent this reorientation and allow for

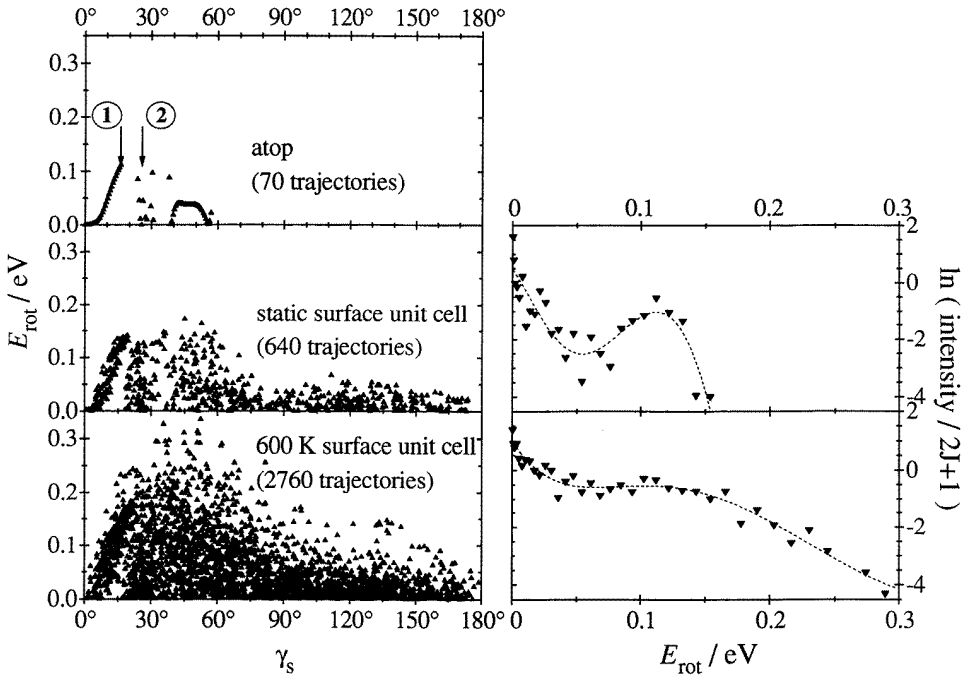

Figure 8. The left-hand panels show the final rotational excitation as a function of the initial orientation angle γ_s of the molecule (γ_s is defined with respect to the surface normal; $\gamma_s = 0$ for the O end towards the surface). The initial energy is 0.3 eV. The impact site of the molecule is at the atop site (with a static surface) and the entire surface unit cell for both the static surface and the 600 K surface. For the atop site, sticking occurs for all molecules with orientation angles beyond 60°. The adjacent right-hand panels show the corresponding Boltzmann plots for the rotational energy distributions. The lines through the Boltzmann plots are merely a guide to the eye. From Lahaye *et al* [79].

rotational rainbow scattering from the O end. The recent work by Lahaye *et al* indicates that such a barrier is not necessary. However, this does not imply that the barrier does not exist, as is apparent from studies by Doren and Tully [82, 83].

The observation of Boltzmann-like distributions in both theoretical and experimental results for NO/Pt(111) suggests extensive randomization of the energy during the collision. Transition state theory then allows us to compute the relative partitioning of the initial energy over the available final states in a statistical fashion. Such an analysis has been applied for NO/Pt(111) [84]. Its turns out that by assuming partial parallel momentum conservation and a decreasing number of surface oscillators (7–10) the experimentally observed angular, energy and rotational state distributions can be explained reasonably well. However, it turned out to be impossible to simultaneously fit all of the different exit channels. Clearly the lifetime of the 'collision complex' is too short to allow for a complete randomization of all accessible exit channels during the lifetime of the local transition state. This time might only be a few hops along the surface. It is surprising that the statistical analysis shows that the angular dependence of the rotational state distribution already vanishes for a very moderate degree of parallel momentum exchange. This has also been seen experimentally in rotational state distributions of CO scattering from (passivated) W(110) [85]. As is

evident from the high sticking probability for NO/Pt(111), in most collisions of NO with the surface complete randomization of the translational energy of the molecule occurs and it gets accommodated to the surface, without being able to desorb.

At incident neutral molecule translational energies exceeding the molecule dissociation energy, molecular dissociation can still have a strong orientation dependence [11, 86]. This may be due to the fact that rotational excitation can be the first step towards dissociation in the so-called centrifugal model [87, 88].

6. Orientation dependence of dissociative chemisorption

The studies on chemisorption of NO on various metal surfaces have demonstrated that there can be a strong orientation dependence of the chemisorption probability. It is very natural to assume that similar effects will also occur for dissociative chemisorption. To date, such studies have not yet been carried out using oriented molecular beams. Only indirect information is available through the dependence of dissociative chemisorption on initial rotational excitation. Such studies have been carried out for the dissociative chemisorption of H_2 on Cu(111) by Rettner, Michelsen and Auerbach [89–92]. It was observed that the initial sticking coefficient at fixed translational energy first decreases with rotational excitation and subsequently increases. The minimum is located at around $J = 3$. These effects have been attributed to an orientation dependence of the sticking coefficient. Other information concerning the orientation dependence of the interaction dynamics can be hidden in the energy dependence of the sticking coefficient. If the barrier to dissociation shows a strong orientation dependence the resulting distribution of barrier heights will give rise to a rather slow rise of the sticking coefficient with energy; see, e.g., [91, 92].

Further information about this can be obtained from a theoretical analysis of the experimental findings. This has been carried out by Darling and Holloway and co-workers. Using a very good theoretical interaction potential the authors find it nevertheless difficult to obtain in a low-dimensional calculation a good agreement with the experimental results [93–95]. This suggests that there is a complicated dependence of the barrier towards dissociation on the lateral position of the molecule and its polar and azimuthal orientation. A two-dimensional representation of the orientation dependence of the interaction is given in figure 9 [93]. Here we plot the position of the classical turning point in the trajectory of a 0.6 eV H_2 molecule, normally incident on a Cu(111) surface along the $\langle -1, -1, 2\rangle$ azimuth, as a function of the molecular orientation and the impact point. The hole around $\pi/2$ and the bridge site indicate that dissociative chemisorption occurs.

7. Molecular orientation and dissociation in fast collisions

7.1. Collisional dissociation mechanisms

Experiments on molecular dissociation induced by impulsive collisions with chemically inert solid surfaces have been performed, e.g. by Gerber and Amirav [96]. Classical trajectory studies on planar, rigid surfaces by the same authors showed that energy transfer to the rotational degree of freedom is very efficient [96]. The angular momentum acquired by the molecule upon impact leads to a reduction in the depth of the intramolecular potential, namely

$$V_J(r) = V_0(r) + J^2/2\mu r^2 \tag{1}$$

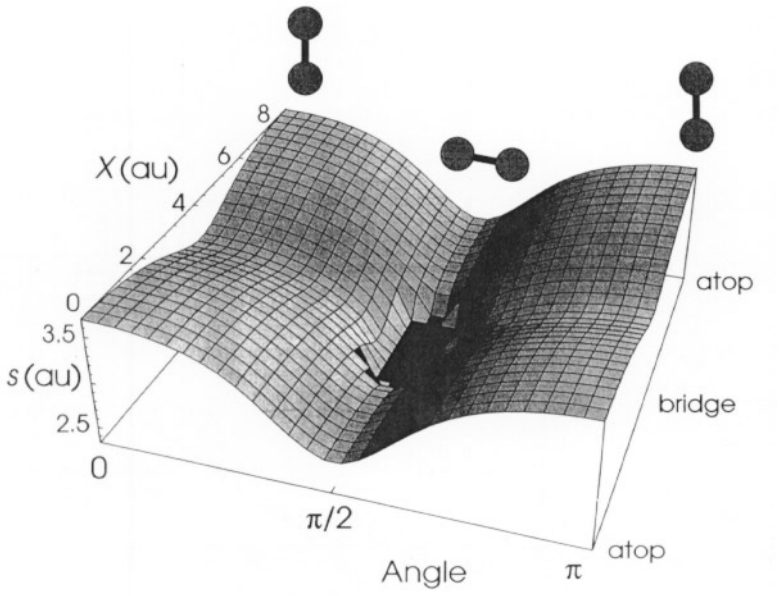

Figure 9. A classical turning surface as a function of molecular orientation and lateral position obtained from trajectory calculations of a 0.6 eV H_2 molecule, normally incident on a Cu(111) surface along the $\langle -1, -1, 2\rangle$ azimuth. It is seen that the fraction that facilitates dissociative adsorption is small (4%). From Kinnersley *et al* [93].

where μ is the reduced mass of the molecule and r the internuclear separation. Dissociation may occur at low J with the assistance of vibrational excitation, which although less efficient, may suffice to overcome the centrifugal barrier. At sufficiently high J, the intramolecular potential (1) becomes purely repulsive and dissociation proceeds unhindered. The simulations showed that rotational excitation was most efficient at intermediate initial molecular-axis orientations θ. This result was also shown to hold for corrugated surfaces by van den Hoek and Kleyn [86], who provided a classical simulation of 1 eV–3 keV O_2 scattering from Ag(111). In a further classical trajectory study by the same group, this time for 70 eV O_2 scattering from Pt(111), Kirchner *et al* [97] showed that early in the interaction, approximately twice as much energy was transferred from the translational to the rotational as to the vibrational degree of freedom, independent of the final outcome of the scattering event. Later in the trajectory, those molecules which finally dissociate were found to possess much more vibrational than rotational energy, while those which do not dissociate have roughly the same amount of energy in vibration and rotation. Unfortunately, the influence of the initial molecular-axis orientation, as opposed to surface structural effects, on this partition of the translational energy between the internal modes was not explicitly investigated.

As the collision energy is increased, the surface appears more corrugated. For 70–200 eV H_2 scattering from Ag(111) at not too large angles of incidence to the surface normal, the dissociation probability was found by van Slooten *et al* [98] to exhibit $E_i\theta_s^2$ scaling, where E_i denotes the incident beam energy and θ_s the total scattering angle of the dissociatively scattered H atoms. This could be understood by assuming that most collisions were governed by the interaction of an incident dumb-bell or ellipsoid-shaped molecule with a single surface atom [99]. If the constituent atoms of the approaching

molecule are well aligned with the surface atom, rotational excitation, and also dissociation, is suppressed [11]. The initial orientation of the molecular axis with respect to the surface normal is of no intrinsic significance.

At very high energies, such as those investigated by Balashova *et al* [100] (30 keV N^{2+} on Cu at 3–10° to the (100) surface plane), the atoms of the molecule and those of the surface appear as point-like particles and the intramolecular interactions are of reduced significance. Molecular-axis orientation effects appear here as well [101, 102], but their origin is trivial. The molecular-axis orientation upon approach to particular surface crystallographic directions determines the probability that either or both atoms of the molecule experience close collisions with atoms of the surface.

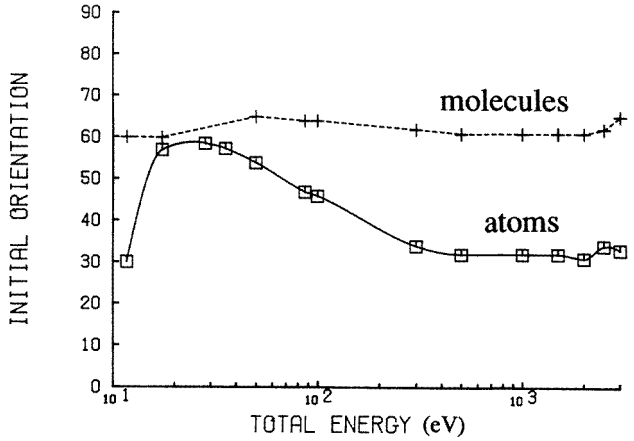

Figure 10. Average initial molecular orientation for O_2 molecules which survive (solid line) and molecules which do not survive (dashed line) the collision with a Ag(111) surface as a function of incident beam energy for a constant surface-normal energy of 11.7 eV and azimuth at 30° to the [110] surface crystallographic direction [86].

If the incidence angle is increased sufficiently toward grazing, shadowing effects eventually become important at all energies. The lateral corrugation of the interaction potential may still be large, but the trajectory of the molecule comes to be dominated by the surface-normal-directed forces experienced by the molecule in passing over the 'peaks' of the corrugated molecule surface interaction potential. Classical trajectory calculations by van den Hoek *et al* [86] have shown that for grazing incidence of 1 eV–3 keV O_2 on Ag(111) and constant surface normal energy of 11.7 eV, the total energy loss and the dissociated fraction each go through a maximum at several tens of eV incident beam energy before becoming independent of energy beyond several hundreds of eV. The average initial orientation of those molecules which survive the collision and those which do not are shown as functions of incident beam energy in figure 10. For high surface-parallel velocities, molecules which survive the collision have flatter initial orientations ($\sim$60°) than molecules which dissociate ($\sim$30°). A simulation of scattering from a truly rigid planar surface gives average initial orientations of 60° and 30° respectively [86], illustrating that for high surface-parallel velocities and glancing incidence, surfaces appear to lose their atomic structure and become 'flat'.

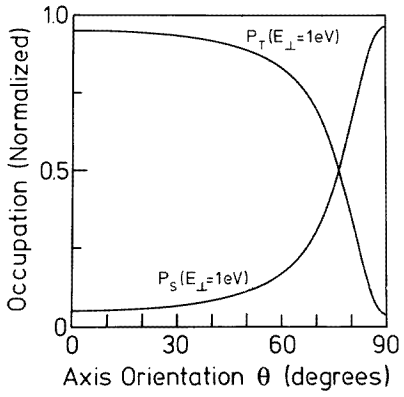

Figure 11. The dependence on the H_2^+ molecular-axis orientation with respect to an Al(110) surface at the instant of charge capture of the probability of capture to the H_2 singlet (S) $X^1\Sigma_g^+$ and triplet (T) $b^3\Sigma_u^+$ states, for an initial internuclear separation in H_2^+ of 2 au and surface-normal beam energy of 1 eV [102].

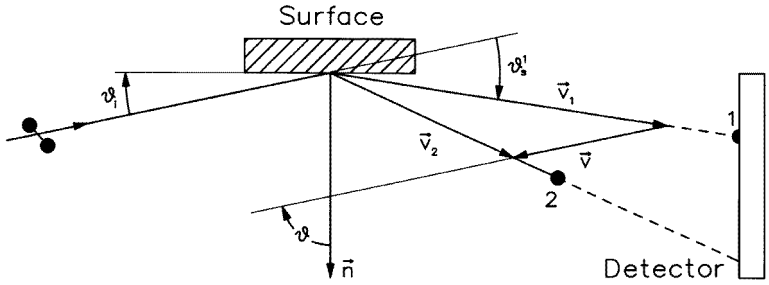

Figure 12. A measurement of the mean velocity, impact position, and arrival time difference of the dissociation fragments of a diatomic molecule defines their relative velocity $\boldsymbol{v} = \boldsymbol{v}_2 - \boldsymbol{v}_1$ to high accuracy [104, 107, 108]. The magnitude v of the relative-velocity vector defines the kinetic energy $\varepsilon = \frac{1}{2}\mu v^2$ in the centre of mass of the molecule, where μ is its reduced mass. For dissociative scattering from a surface it is convenient to give the final orientation θ of the vector $\boldsymbol{v}$ with reference to the surface normal, $\boldsymbol{n}$. The orientation θ is identical to the final orientation of the internuclear coordinate. The technique can distinguish between dissociative scattering events in which fragment 2 lags behind fragment 1 ('backward-leaning' final molecular-axis orientations, for which we assign positive values of θ, as for the event shown) and events in which fragment 2 leads fragment 1 ('forward-leaning' events, for which we assign negative θ-values).

7.2. Electronic dissociation mechanisms

Beyond the physisorption regime, charge transfer dominates the interaction of a slow molecule with the surface of a metal. It often leads to the making of bonds between the atoms of the molecule and the surface and to the breaking of bonds within the molecule. Such charge rearrangements are a consequence of the spatial overlap of electronic states ψ_m of the molecule with conduction band states ψ_k of the metal. The electronic matrix element describing the transition of an electron between ψ_k and ψ_m can be written in the form

$$V_{mk} = \langle \psi_m | V | \psi_k \rangle \tag{2}$$

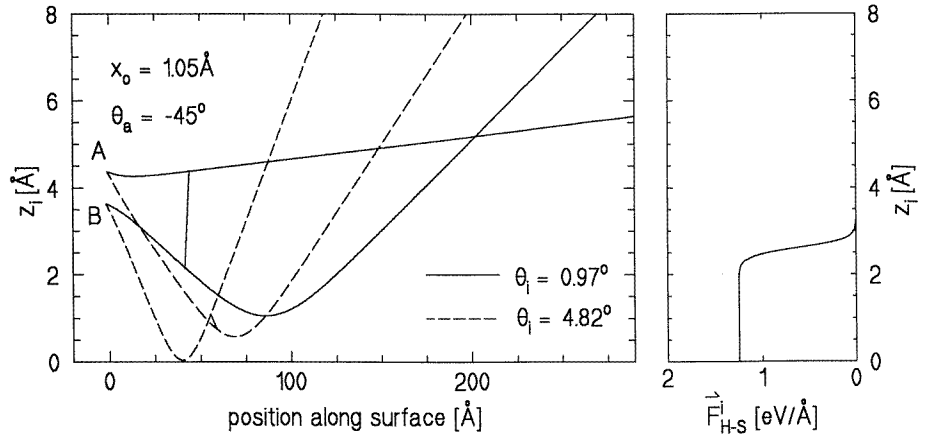

Figure 13. Calculated trajectories of H atoms, assuming dissociation of a 3 keV hydrogen molecule on a potential surface constructed from purely repulsive pair potentials of the form $V_{H-H}(x) = V^0_{H-H}\exp(-\alpha_{H-H}x)$ and $V_{H-S}(z_i) = V^0_{H-S}\exp(-\alpha_{H-S}z_i)$ with the parameters given in [105]. The dissipative interaction of each atom with the surface is described by the z-dependent friction force shown on the right and directed antiparallel to the direction of motion of each atom. The parameters have been chosen to reproduce the mean energy losses observed experimentally for 3 keV H_2^+ scattering from Cu(111). At small glancing angles Θ_i of the beam to the surface and not too large initial molecular-axis orientations $|\theta_a|$, the upper atom A interacts only weakly with the surface and suffers very little energy loss. For larger values of $|\theta_a|$ and/or Θ_i both atoms interact strongly with the surface.

where the operator V describes the interaction between the electron and the molecule. The absence of spherical symmetry in the molecule leads to an orientation dependence of both the transition matrix element and the associated charge-transfer rate [101–104]. If the incident molecule is positively ionized, and charge transfer to non-bonding states of the neutral molecule is energetically possible, an orientation dependence for dissociative scattering is conceivable. A concrete example is provided by the H_2^+ molecule. Upon approach to a metal surface, both the singlet $X^1\Sigma_g^+$ and triplet $b^3\Sigma_u^+$ states of H_2 are generally considered to be accessible for charge transfer. The expected dependence on molecular-axis orientation of the probability of charge capture into these states at an Al(110) surface is reproduced in figure 11. The experimental verification of such orientation dependencies is problematic. Adiabaticity arguments suggest that charge transfer occurs as the molecule approaches the surface. If the surface were to act as a perfect, planar mirror, a measurement of the final orientation θ of the internuclear coordinate of the scattered fragments would provide direct information on the orientation dependence of dissociative charge transfer to the triplet state†. However, as pointed out by Imke *et al* [106] and Schins *et al* [104], the interaction of the fragments with the surface following charge transfer cannot in general be neglected. At particle velocities where a measurement of θ is experimentally feasible using the technique of translational spectroscopy ([104, 107, 108] and figure 12), strong dissipative (friction-like) forces significantly modify the particle trajectories (figure 13).

Internuclear coordinate orientation distributions have been directly measured for dissociative scattering of H_2^+ from Cu(111) over the incident-beam translational energy

† Neglecting H–H scattering, an initial orientation θ (at the instant charge transfer to the dissociative state occurs) maps to the final orientation $-\theta$ (see figure 9 of [105]).

range $E_i = 500$ eV–6 keV and normal energy range 0.2–8 eV [105]. Results for $E_i = 3$ keV are shown in the upper panel of figure 14. These results are consistent with the picture that at low surface-normal beam energies, only one fragment of the molecule interacts strongly with the surface, slowing it down (figure 13). This factor, combined with the larger scattering angle of this fragment (figure 13), leads naturally to the observed 'backward-leaning' scattered-fragment orientation distribution (see the upper left-hand panel of figure 14). At higher surface-normal beam energies, both fragments of the molecule interact strongly with the surface (figure 13). In this case, apart from some smearing, the final orientation distribution should more accurately reflect the molecular-axis orientation distribution immediately after charge transfer to the unbound triplet state†. No evidence for the expected depletion (figure 11) of surface-parallel orientations is, however, observed in the experiment (see the upper right-hand panel of figure 14). In fact, a classical simulation is able to reproduce the essential features of the observed spectra at all surface-normal beam energies by assuming an isotropic orientation distribution in the triplet state immediately following charge transfer [105]. One possible reason for this apparent discrepancy is that the singlet state is not strongly populated during scattering of fast H_2^+ from Cu(111)†. The matrix element for charge transfer to the triplet state will of course still exhibit an orientation dependence, as would the charge-transfer rate or resonance width. However, in the absence of strongly competing charge-transfer channels, at low surface-normal velocities the triplet-state occupation could conceivably saturate [104] at unity, independent of the molecular-axis orientation.

Incident neutral molecules or initially ionized molecules which neutralize to a bound state can still dissociatively scatter [109–111], even under conditions where the collisional mechanisms discussed in the preceding subsection are suppressed. Fast neutral H_2 in its ground electronic state is efficiently dissociated in grazing collisions with metal surfaces [110, 111]. The scattered-fragment internuclear-axis orientation distributions of H_2 scattered from Cu(111) [111] are in fact almost indistinguishable from those of H_2^+ (the upper and centre panels of figure 14). If our interpretation of the origin of the structures observed in the upper panel of figure 14 is correct, then we are inclined to conclude that at least the entrance channel topographies of the potential energy surfaces (PES) governing the interaction of H_2 $X^1\Sigma_g^+$ and H_2 $b^3\Sigma_u^+$ with Cu(111) are very similar [111]. However, the topography of the adiabatic ground state of the H_2/Cu(111) system is now quite well established [112]. The H–H interaction is by no means purely repulsive in the pre-barrier region of the ground-state PES. Since a repulsive H–H interaction during the approach of the molecule to the surface is crucial in producing the characteristic θ-dependencies seen in the upper panel of figure 14, we conclude that the dynamics of the interaction of fast neutral H_2 with Cu(111) is influenced by additional (higher-lying) potential surfaces with topography quite different to that of the adiabatic ground state.

How are such states accessed during the interaction? We recollect our earlier observation that the interaction of a fast beam with a surface under glancing-incidence conditions is strongly dissipative. Converting the experimentally measured total translational energy losses to losses per unit time in the interaction region [111], we discover that energy is dissipated at rates in the 0.1–1 eV fs^{-1} regime. Most of the energy appears to be

† The result shown in figure 11 is for charge capture to H_2^+ from Al(110). In this case the gas-phase $X^1\Sigma_g^+$ and $b^3\Sigma_u^+$ states of H_2 lie energetically between the bottom of the conduction band and the Fermi level, and both resonant and Auger transitions can contribute to the population of each state. For Cu(111), the gas-phase $X^1\Sigma_g^+$ state lies well below the bottom of the conduction band. In the absence of a large upward shift of this state, resonant coupling to the conduction band is prevented. The suppression of this charge-transfer channel would presumably lead to an enhanced population of the competing triplet state.

transferred to the metal conduction electrons via an efficient electron–hole pair excitation mechanism [113]. The resulting 'hot' electrons are therefore continuously available to populate higher-lying electronic states of the molecule–metal system.

The signature of such processes in the scattered-fragment orientation distributions is influenced by both the topographies of the participating PESs and the effective contributions of each to the nuclear dynamics. This is illustrated in the centre and lower panels of figure 14, where experimental results for the dissociative scattering of neutral H_2 and D_2, which of course are governed by identical PESs, are compared. The lower surface-parallel velocity of D_2 leads to a lower rate of energy dissipation [114]. As a consequence, fewer 'hot' electrons are available to populate higher-lying electronic states of the system. The influence of the topography of the corresponding upper-state PES is therefore reduced. The essential features and the observed changes in the orientation distributions (figure 14) have been successfully reproduced by a classical simulation of the above scenario using PESs appropriate for the H_2/D_2/Cu(111) system [115].

Fragment orientation distributions of the molecules N_2, NO and their positive ions N_2^+ and NO^+ dissociatively scattered from Cu(111) and Pt(111) are sharply peaked about $\theta = 0^\circ$. The adsorption of N_2 on Cu(111) is known to be highly activated [116], while that of NO is at most only weakly activated [117]. Despite this significant difference in adiabatic ground-state PES topography for the two molecules on Cu(111), the fragment orientation distributions are almost identical (figure 15). We must look elsewhere for the origin of the strong surface-normal-oriented fragment distributions.

An orientation $\theta \simeq 0^\circ$ implies that during the interaction of the molecule with the surface, the accumulated difference in the surface-parallel velocity components of the two atoms is smaller than the accumulated difference in the surface-normal velocity components. These velocity differences arise from corresponding differences in the force components acting on the two atoms. The above-mentioned weak expression of seemingly important topographical features of the ground-state PES encourages us once again to explore the influence of a transient population of higher-lying electronic states of the molecule–surface system during the interaction. We have examined the influence of a variety of lower- and upper-state PES topographies on the dissociative scattering dynamics. We find that we can reproduce the observed surface-normal-oriented fragment pair distribution in simulations where dissociation occurs via potential surface-hopping-induced vibrational excitation of the molecule in the entrance channel region of the adiabatic ground-state PES [115]. The same mechanism leads to a high surface-normal orientational preference of the vibrationally excited non-dissociatively scattered molecules. This latter prediction is yet to be verified experimentally.

8. Conclusions

The role of the orientation of a molecule in its interaction with a surface has been examined for a number of cases: adsorbed molecules, scattered molecules, reacting molecules, molecules that dissociatively chemisorb at the surface, and molecules that dissociate in a fast collision. In all cases the molecular orientation is seen to be an important degree of freedom. It has a strong influence on the dynamics of the interaction. The orientation dependence of quantities like scattered or adsorbed flux can cause intensity variations of 0.1 to 10. In certain orientations sticking, scattering and dissociation are not possible at all.

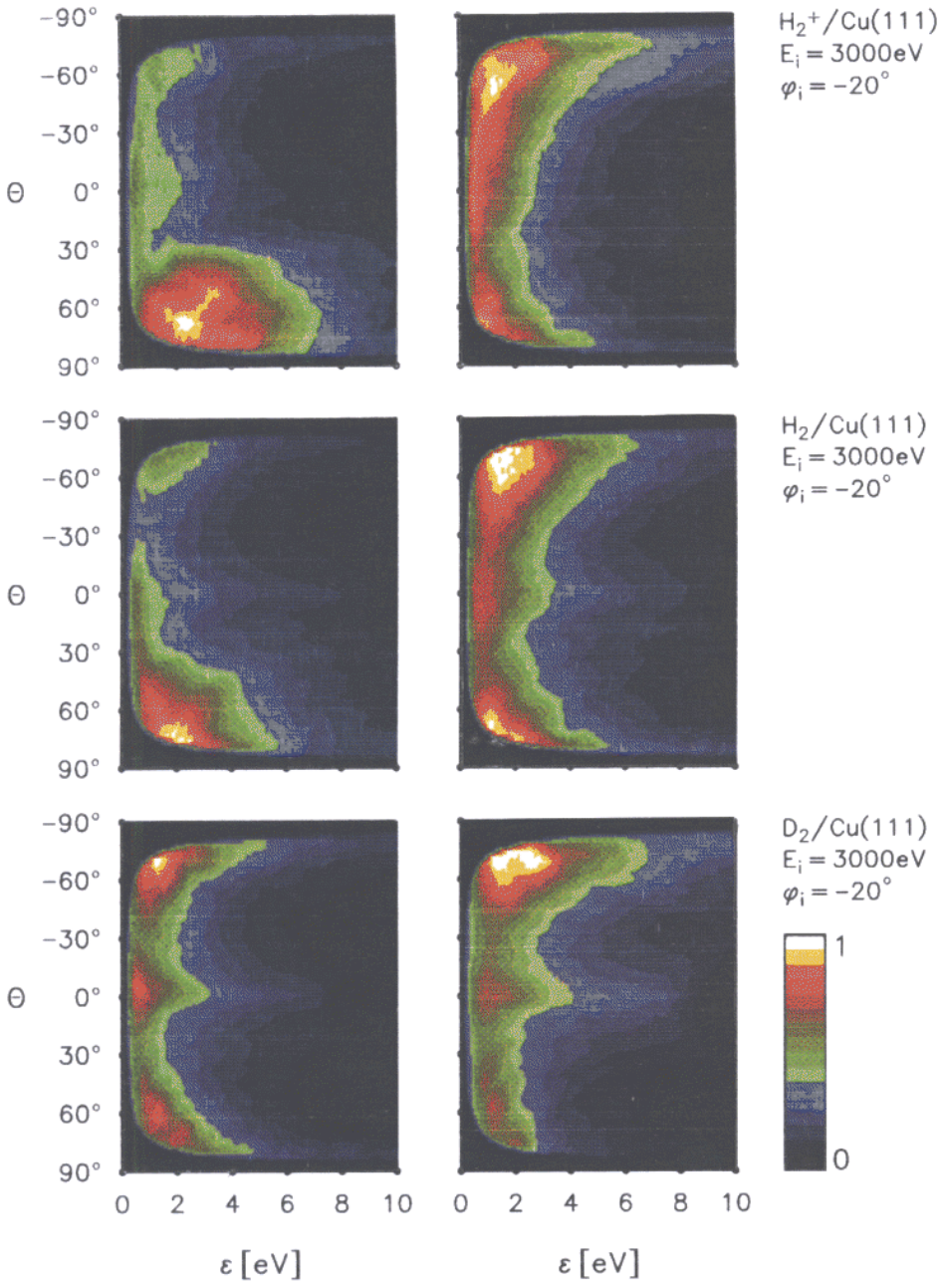

Figure 14. The dependence on the surface-normal beam energy $E_{\perp i}$ (left, 0.7 eV; right, 4.0 eV) and incident molecular species (H_2^+, H_2 and D_2) of the normalized distributions of the number of dissociative scattering events recorded (in the plane containing the incident beam and the surface normal) at the centre-of-mass kinetic energy ε and internuclear coordinate orientation θ (see figure 3). The beam was in all cases incident at an azimuthal angle of 20° to the [110] direction of the Cu(111) crystal. The linear height scale is defined on the right. The black region close to the ε- and θ-axes is blind to the detector.

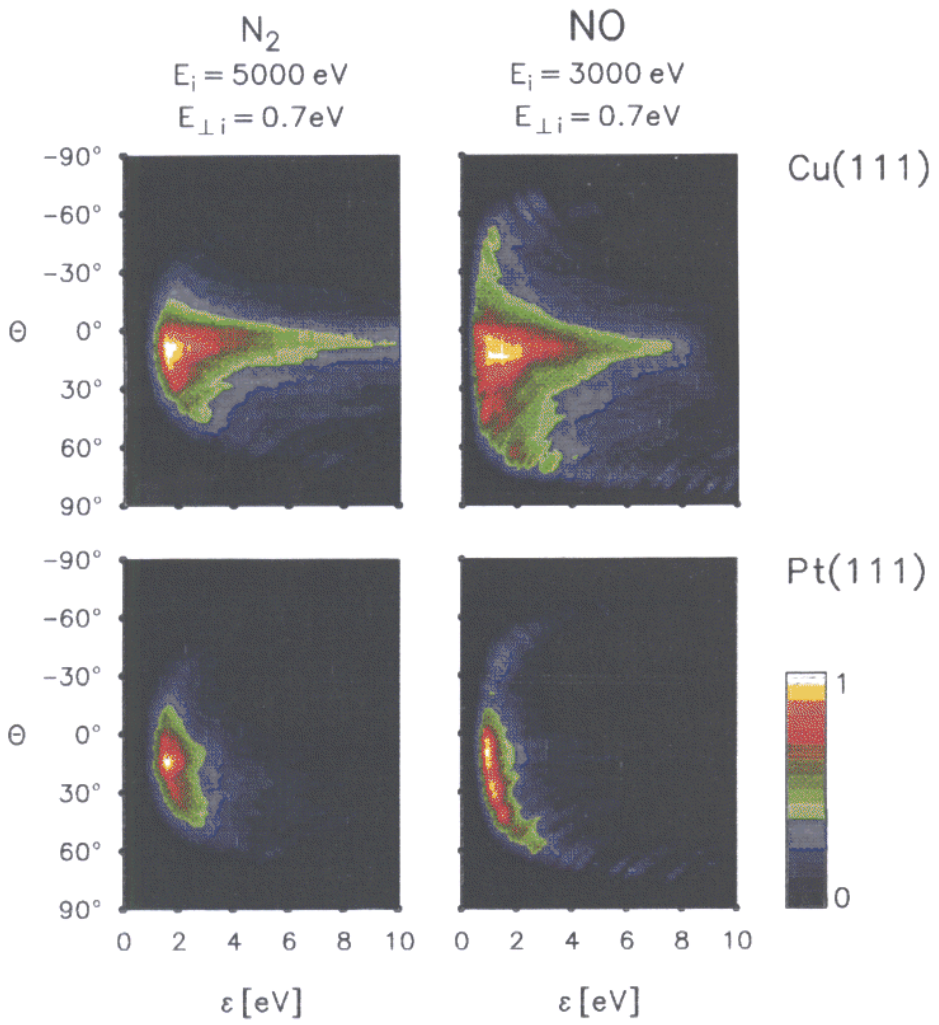

Figure 15. The dependence on the incident molecular species (N_2 and NO) and surface (Cu(111) and Pt(111)) of the normalized distributions of the number of dissociative scattering events recorded (in the plane containing the incident beam and the surface normal) at the centre-of-mass kinetic energy ε and internuclear coordinate orientation θ (see figure 12). The beam was in all cases incident at an azimuthal angle of 20° to the [110] direction of the (111) crystal surface. The linear height scale is defined on the right. The black region close to the ε- and θ-axes is blind to the detector.

Acknowledgments

The work described in this review is in part the result of a collaboration of the authors and their research groups supported by the network on 'Orientation in molecule–surface interactions' of the EU Science Plan (Contract SC1*-CT91-0721).

References

[1] Ibach H and Mills D L 1982 *Electron Energy Loss Spectroscopy and Surface Vibrations* (New York: Academic)
[2] Stöhr J 1992 *NEXAFS Spectroscopy* (Berlin: Springer)
[3] Rous P J 1992 *Prog. Surf. Sci.* **39** 3
[4] Kleyn A W, Luntz A C and Auerbach D J 1981 *Phys. Rev. Lett.* **47** 1169
[5] Kleyn A W, Luntz A C and Auerbach D J 1982 *Surf. Sci.* **117** 33
[6] Sitz G O, Kummel A C and Zare R N 1988 *J. Chem. Phys.* **89** 2558
[7] Sitz G O, Kummel A C, Zare R N and Tully J C 1988 *J. Chem. Phys.* **89** 2572
[8] Hines M A and Zare R N 1993 *J. Chem. Phys.* **98** 9134
[9] Kuipers E W, Tenner M G, Kleyn A W and Stolte S 1988 *Nature* **334** 420
[10] Holloway S and Jackson B 1990 *Chem. Phys. Lett.* **172** 40
[11] van Slooten U and Kleyn A W 1993 *Chem. Phys.* **177 509**
[12] Vattuone L, Boragno C, Pupo M, Restelli P, Rocca M and Valbusa U 1994 *Phys. Rev. Lett.* **72** 510
[13] Vattuone L, Rocca M, Restelli P, Pupo M, Boragno C and Valbusa U 1994 *Phys. Rev.* B **49** 5113
[14] Vattuone L, Rocca M, Boragno C and Valbusa U 1994 *J. Chem. Phys.* **101** 713
[15] Vattuone L, Rocca M, Boragno C and Valbusa U 1994 *J. Chem. Phys.* **101** 726
[16] Spruit M E M, van den Hoek P J, Kuipers E W, Geuzebroek F H and Kleyn A W 1989 *Surf. Sci.* **214** 591
[17] Spruit M E M, Kuipers E W, Geuzebroek F H and Kleyn A W 1989 *Surf. Sci.* **215** 421
[18] Spruit M E M and Kleyn A W 1989 *Chem. Phys. Lett.* **159** 342
[19] Raukema A and Kleyn A W 1995 *Phys. Rev. Lett.* **74** 4333
[20] Raukema A, Dirksen R J and Kleyn A W 1995 *J. Chem. Phys.* **103** 6217
[21] Raukema A, Butler D A, Box F M A and Kleyn A W 1996 *Surf. Sci.* **347** 151
[22] Raukema A, Butler D A and Kleyn A W 1996 *J. Phys.: Condens. Matter* **8** 2247
[23] Guest R J, Hernnas B, Bennich P, Björneholm O, Nilsson A, Palmer R E and Mårtensson N 1992 *Surf. Sci.* **278** 239
[24] Besenbacher F and Nørskov J K 1993 *Prog. Surf. Sci.* **44** 1
[25] Outka D A, Stöhr J, Jark W, Stevens P, Solomon J and Madix R J 1987 *Phys. Rev.* B **35** 4119
[26] Barnard J C, Bug A and Palmer R E 1996 to be published
[27] Guest R J, Goldby I M, Palmer R E, Bly D N, Hartley D M and Rous P J 1993 *Faraday Discuss.* **96** 117
[28] Palmer R E 1992 *Prog. Surf. Sci.* **41** 51
[29] Palmer R E and Rous P J 1992 *Rev. Mod. Phys.* **64 383**
[30] Ramsier R D and Yates J T 1991 *Surf. Sci. Rep.* **12** 243
[31] Fecher G, Böwering N, Volkmer M, Pawlitzky B and Heinzmann U 1990 *Surf. Sci.* **230** L169
[32] Tenner M G, Kuipers E W, Langhout W Y, Kleyn A W, Nicolasen G and Stolte S 1990 *Surf. Sci.* **236** 151
[33] Müller H, Dierks B, Hamza F, Zagatta G, Fecher G H, Böwering N and Heinzmann U 1992 *Surf. Sci.* **269/270** 207
[34] Geuzebroek F H, Wiskerke A E, Tenner M G, Kleyn A W, Stolte S and Namiki A 1991 *J. Phys. Chem.* **95** 8409
[35] Brandt M, Müller H, Zagatta G, Wehmeyer O, Böwering N and Heinzmann U 1995 *Surf. Sci.* **333** 30
[36] King D A and Wells M G 1972 *Surf. Sci.* **29** 454
[37] Müller H, Zagatta G, Böwering N and Heinzmann U 1994 *Chem. Phys. Lett.* **223** 197
[38] Tenner M G, Kuipers E W, Kleyn A W and Stolte S 1988 *J. Chem. Phys.* **89** 6552
[39] Kleyn A W, Kuipers E W, Tenner M G and Stolte S 1989 *J. Chem. Soc. Faraday Trans.* II **85** 1337
[40] Kuipers E W, Tenner M G, Kleyn A W and Stolte S 1989 *Surf. Sci.* **211/212** 819
[41] Kuipers E W, Tenner M G, Kleyn A W and Stolte S 1989 *Phys. Rev. Lett.* **62** 2152
[42] Kuipers E W, Tenner M G, Kleyn A W and Stolte S 1989 *Chem. Phys.* **138** 451
[43] Kuipers E W, Tenner M G, Kleyn A W and Stolte S 1990 *J. Vac. Sci. Technol.* A **8** 2692
[44] Tenner M G, Geuzebroek F H, Kuipers E W, Kleyn A W, Stolte S and Namiki A 1990 *Chem. Phys. Lett.* **168** 45
[45] Tenner M G, Kuipers E W, Kleyn A W and Stolte S 1991 *J. Chem. Phys.* **94** 5197
[46] Geuzebroek F H, Wiskerke A E, Kleyn A W and Stolte S 1991 *Nucl. Instrum. Methods Phys. Res.* B **58** 354
[47] Müller H, Dierks B, Fecher G H, Böwering N and Heinzmann U 1994 *J. Chem. Phys.* **101** 7154
[48] Müller H, Zagatta G, Brandt M, Wehmeyer O, Böwering N and Heinzmann U 1994 *Surf. Sci.* **309** 159
[49] Kuipers E W, Tenner M G, Spruit M E M and Kleyn A W 1988 *Surf. Sci.* **205** 241
[50] Müller H, Zagatta G, Brandt M, Bennett R A, Böwering N and Heinzmann U 1995 *Proc. Symp. on Surface*

Science (Kaprun, 1995) (Vienna: TU Wien Press) 3S 95, p 219
[51] Zagatta G, Müller H, Böwering N and Heinzmann U 1994 *Rev. Sci. Instrum.* **65** 359
[52] Zagatta G, Müller H, Wehmeyer O, Brandt M, Böwering N and Heinzmann U 1994 *Surf. Sci.* **309** 199
[53] Harris J and Kasemo B 1981 *Surf. Sci.* **105** L281
[54] LaVilla M E and Ionov S I 1991 *J. Chem. Phys.* **95** 5486
[55] LaVilla M E and Ionov S I 1992 *Phys. Rev. Lett.* **68** 129
[56] LaVilla M E, Ionova I V and Ionov S I 1992 *J. Chem. Phys.* **97** 9366
[57] LaVilla M E and Ionov S I 1992 *J. Chem. Phys.* **97** 9379
[58] Ionov S I and Bernstein R B 1991 *J. Chem. Phys.* **94** 1564
[59] Curtiss T J, Mackay R S and Bernstein R B 1990 *J. Chem. Phys.* **93** 7387
[60] Ionov S I, LaVilla M E and Bernstein R B 1990 *J. Chem. Phys.* **93** 7416
[61] Ionov S I, LaVilla M E, Mackay R S and Bernstein R B 1990 *J. Chem. Phys.* **93** 7406
[62] Curtiss T J and Bernstein R B 1989 *Chem. Phys. Lett.* **161** 212
[63] Tenner M G, Kuipers E W, Kleyn A W and Stolte S 1991 *Surf. Sci.* **242** 376
[64] Hand M R, Chang X Y and Holloway S 1990 *Chem. Phys.* **147** 351
[65] Kleyn A W 1987 *Comment. At. Mol. Phys.* **19** 133
[66] Kleyn A W and Horn T C M 1991 *Phys. Rep.* **199** 191
[67] Kleyn A W 1994 *Surf. Rev. Lett.* **1** 157
[68] Korsch H J and Ernesti A 1992 *J. Phys. B: At. Mol. Phys.* **25** 3565
[69] Brown J K and Luntz A C 1993 *Chem. Phys. Lett.* **204** 451
[70] Materer N, Barbieri A, Gardin D, Starke U, Batteas J D, van Hove M A and Somorjai G A 1994 *Surf. Sci.* **303** 319
[71] Jacobs D C, Kolasinski K W, Shane S F and Zare R N 1989 *J. Chem. Phys.* **91** 3182
[72] Jacobs D C and Zare R N 1989 *J. Chem. Phys.* **91** 3196
[73] Haug C, Brenig W and Brunner T 1992 *Surf. Sci.* **265** 56
[74] Wiskerke A E, Taatjes C A, Kleyn A W, Lahaye R J W E, Stolte S, Bronnikov D K and Hayden B E 1993 *Chem. Phys. Lett.* **216** 93
[75] Wiskerke A E, Taatjes C A, Kleyn A W, Lahaye R J W E, Stolte S, Bronnikov D K and Hayden B E 1993 *Faraday Discuss.* **96** 297
[76] Wiskerke A E, Taatjes C A, Kleyn A W, Lahaye R J W E, Stolte S, Bronnikov D K and Hayden B E 1995 *J. Chem. Phys.* **102** 3835
[77] Wiskerke A E and Kleyn A W 1995 *J. Phys.: Condens. Matter* **7** 5195
[78] Harris J and Luntz A C 1989 *J. Chem. Phys.* **91** 6421
[79] Lahaye R J W E, Stolte S, Holloway S and Kleyn A W 1996 *J. Chem. Phys.* **104** at press
[80] Horn T C M, Kleyn A W and Gislason E A 1988 *Chem Phys.* **127** 81
[81] Lahaye R J W E, Kleyn A W, Stolte S and Holloway S 1995 *Surf. Sci.* **338** 169
[82] Doren D J and Tully J C 1991 *J. Chem. Phys.* **94** 8428
[83] Doren D J and Tully J C 1988 *Langmuir* **4** 256
[84] Taatjes C A, Wiskerke A E and Kleyn A W 1995 *J. Chem. Phys* **102** 3848
[85] Hanisco T F and Kummel A C 1993 *J. Chem. Phys.* **99** 7076
[86] van den Hoek P J and Kleyn A W 1989 *J. Chem. Phys.* **91** 4318
[87] Gerber R B and Elber R 1984 *Chem. Phys. Lett.* **107** 141
[88] Gerber R B and Elber R 1983 *Chem. Phys. Lett.* **102** 466
[89] Michelsen H A, Rettner C T, Auerbach D J and Zare R N 1993 *J. Chem. Phys.* **98** 8294
[90] Michelsen H A, Rettner C T and Auerbach D J 1992 *Phys. Rev. Lett.* **69** 2678
[91] Rettner C T, Michelsen H A and Auerbach D J 1995 *J. Chem. Phys.* **102** 4625
[92] Michelsen H A, Rettner C T and Auerbach D J 1994 The adsorption of hydrogen at copper surfaces–a model system for the study of activated adsorption *Surface Reactions* ed R J Madix (Berlin: Springer) p 185
[93] Kinnersley A D, Darling G R, Holloway S and Hammer B 1996 *Surf. Sci.* submitted
[94] Darling G R and Holloway S 1993 *Faraday Discuss.* **96** 43
[95] Darling G R and Holloway S 1994 *J. Chem. Phys.* **101** 3268
[96] Gerber R B and Amirav A 1986 *J. Phys. Chem.* **90** 4483
[97] Kirchner E J J, Baerends E J, van Slooten U and Kleyn A W 1992 *J. Chem. Phys.* **97** 3821
[98] van Slooten U, Andersson D, Kleyn A W and Gislason E A 1991 *Chem. Phys. Lett.* **185** 440
[99] van Slooten U, Andersson D R, Kleyn A W and Gislason E A 1992 *Surf. Sci.* **274** 1
[100] Balashova L L, Garin S N, Dodonov A I, Mashkova E S and Molchanov V A 1982 *Surf. Sci.* **119** L378
[101] Imke U, Snowdon K J and Heiland W 1986 *Phys. Rev.* B **34** 48

[102] Imke U, Snowdon K J and Heiland W 1986 *Phys. Rev.* B **34** 41
[103] Gadzuk J W 1987 *Surf. Sci.* **180** 225
[104] Schins J, Vrijen R B, van der Zande W J and Los J 1993 *Surf. Sci.* **280** 145
[105] Harder R, Nesbitt A, Herrmann G, Tellioglu K, Rechtien J H and Snowdon K J 1994 *Surf. Sci.* **316** 63
[106] Imke U, Schubert S, Snowdon K J and Heiland W 1987 *Surf. Sci.* **189/190** 960
[107] De Bruijn D P and Los J 1982 *Rev. Sci. Instrum.* **53** 1020
[108] Rechtien J H, Harder R, Herrmann G, Nesbitt A, Tellioglu K and Snowdon K J 1993 *Surf. Sci.* **282** 137
[109] Reijnen P H F, van Slooten U and Kleyn A W 1991 *J. Chem. Phys.* **94** 695
[110] Schmidt K, Franke H, Närmann A and Heiland W 1992 *J. Phys.: Condens. Matter* **4** 9869
[111] Harder R, Nesbitt A, Golichowski A, Herrmann G and Snowdon K J 1994 *Surf. Sci.* **316** 47
[112] Hammer B, Scheffler M, Jacobsen K W and Norskov J K 1994 *Phys. Rev. Lett.* **73** 1400
[113] Bilic A, Gumhalter B, Mix W, Golichowski A, Tzanev S and Snowdon K J 1994 *Surf. Sci.* **309** 165
[114] Nesbitt A, Harder R, Golichowski A, Herrmann G and Snowdon K J 1994 *Chem. Phys.* **179** 215
[115] Snowdon K J, Harder R and Nesbitt A 1996 *Surf. Sci.* at press
[116] Higgs V, Hollins P, Pemble M E and Pritchard J 1986 *J. Electron Spectrosc. Relat. Phenom.* **39** 137
[117] Balkenende A R, Gijzeman O L J and Geus J W 1989 *Appl. Surf. Sci.* **37** 189